

Experimental generation and characterization of single-photon hybrid ququarts based on polarization and orbital angular momentum encoding

Eleonora Nagali,¹ Linda Sansoni,¹ Lorenzo Marrucci,^{2,3} Enrico Santamato,^{2,4} and Fabio Sciarrino^{1,5,*}

¹*Dipartimento di Fisica, Sapienza Università di Roma, Roma I-00185, Italy*

²*Dipartimento di Scienze Fisiche, Università di Napoli “Federico II”, Complesso Universitario di Monte S. Angelo, I-80126 Napoli, Italy*

³*CNR-SPIN, Coherencia, Complesso Universitario di Monte S. Angelo, I-80126 Napoli, Italy*

⁴*Consorzio Nazionale Interuniversitario per le Scienze Fisiche della Materia, I-80126 Napoli, Italy*

⁵*Istituto Nazionale di Ottica, Largo Fermi 6, I-50125 Firenze, Italy*

(Received 27 January 2010; published 14 May 2010)

High-dimensional quantum states, or *qudits*, represent a promising resource in the quantum information field. Here we present the experimental generation of four-dimensional quantum states, or *ququarts*, encoded in the polarization and orbital angular momentum of a single photon. Our technique, based on the q -plate device, allows the ququart to be prepared and measured in all five mutually unbiased bases. We report the reconstruction of the four-dimensional density matrix through the tomographic procedure for different ququart states.

DOI: [10.1103/PhysRevA.81.052317](https://doi.org/10.1103/PhysRevA.81.052317)

PACS number(s): 42.50.Ex, 03.67.—a

I. INTRODUCTION

In quantum information theory, the fundamental unit of information is a two-level system, the qubit. As in classical information science, in principle, all quantum information tasks can be performed based only on qubits and on quantum gates working on qubits. For practical reasons, however, there may be a significant advantage in introducing the use of higher-dimensional systems for encoding and manipulating the quantum information. Such d -level quantum systems, or *qudits*, provide a natural extension of qubits that has been shown to be suitable for prospective applications such as quantum cryptography and computation [1,2]. The growing interest in qudit states lies in two main aspects. On one hand, the adoption of multidimensional states has been proven to increase the efficiency of Bell-state measurements for quantum teleportation and to enhance the violation of Bell-type inequalities [3–7]. On the other hand, besides implications in fundamental quantum mechanics theory [8], the qudit offers several advantages in the field of quantum information [9–11]. Indeed, d -dimensional states are more robust against isotropic noise and, hence, offer higher transmission rates through communication channels [12,13]. Several quantum cryptographic protocols have been developed in order to capitalize on the usefulness of these states, especially their capability to increase security against eavesdropping attacks and the noise threshold that quantum key distribution protocols can tolerate [1,14–22]. Furthermore, qudits also offer advantages for more efficient quantum gates [23] and for quantum information protocols [24,25].

In the past few years, many different implementations of qudits have been proposed and demonstrated (see, e.g., [26,27]). In quantum optics, implementations of *qutrit* ($d = 3$) and *ququart* ($d = 4$) states have been carried out, for example, by exploiting two-photon polarization states [28–30]. In such cases, a natural basis for the ququart Hilbert space of a photon pair is the following: $\{|H_a, H_b\rangle, |H_a, V_b\rangle, |V_a, H_b\rangle, |V_a, V_b\rangle\}$, where H and V refer to the horizontal and vertical linear

polarization states, and a and b denote the two photon modes. Hence, a pair of photons can be exploited to encode a ququart state. When the two modes coincide ($a = b$), a qutrit system is obtained since the two states $|H_a, V_b\rangle$ and $|V_a, H_b\rangle$ become indistinguishable. Different experiments on biphoton qudits have been performed by adopting the spontaneous parametric down-conversion process: preparation and measurement of ququarts encoded in polarization and frequency degrees of freedom [31,32], realization of polarization qutrit from non-maximally entangled states [33], and entanglement between ququart systems [34]. A biphoton implementation, however, has several limitations. First of all, the rotated basis of the ququarts corresponds to entangled states of the biphoton. Furthermore, the implementation of unitary operation on a single quantum system requires an interaction between two photons, a task that can be achieved only probabilistically with linear optics. Finally, the detection efficiency scales as η^2 , where η includes transmission losses and detection efficiency; thus, low implementation rates are typically achieved.

An alternative approach to realize photon qudits is that based on degrees of freedom other than polarization, within a single photon. In this context, a particularly attractive choice is the orbital angular momentum (OAM) of light, which provides a natural discrete high-dimensional basis of photon quantum states within a given longitudinal optical mode [35–37]. Up to now, qudits with $d = 3$ and $d = 4$ encoded in photonic purely OAM systems have been generated [38,39] and employed in quantum communication [40], quantum coin tossing [41], quantum bit commitment [42], and quantum key distribution [18]. However, despite its many potential advantages, the use of OAM so far has been limited by technical difficulties arising in the full manipulation and transmission of this degree of freedom. For example, in contrast to polarization, OAM coherent superpositions are affected by simple free-space propagation, owing to the different Gouy phases associated with different OAM values.

In the present paper, we manipulate the polarization and OAM degrees of freedom to generate a ququart encoded in a single photon. Since we exploit two different degrees of freedom of the same particle, we refer to *hybrid* ququart states. Such results have been achieved through the q -plate

*fabio.sciarrino@uniroma1.it

device [43,44], which couples the spinorial (polarization) and orbital contributions of the angular momentum of photons. A complete characterization of the ququart states has been carried out by the quantum-state tomography technique.

II. QUQUART REALIZATION

Let us consider the bidimensional OAM subspace with $m = \pm 2$, where m denotes the OAM per photon along the beam axis in units of \hbar . We denote such subspace as $o_2 = \{|+2\rangle, |-2\rangle\}$. According to the nomenclature $|\varphi, \phi\rangle = |\varphi\rangle_\pi |\phi\rangle_{o_2}$, where $|\cdot\rangle_\pi$ and $|\cdot\rangle_{o_2}$ stand for the photon quantum state “kets” in the polarization and OAM degrees of freedom, the logic ququart basis

$$\{|1\rangle, |2\rangle, |3\rangle, |4\rangle\}$$

can be rewritten as

$$\{|H, +2\rangle, |H, -2\rangle, |V, +2\rangle, |V, -2\rangle\},$$

where H (V) refers to horizontal (vertical) polarization. Following the same convention, the OAM equivalent of the two basis linear polarizations $|H\rangle$ and $|V\rangle$ are then defined as

$$\begin{aligned} |h\rangle &= \frac{1}{\sqrt{2}}(|+2\rangle + |-2\rangle) \\ |v\rangle &= \frac{1}{i\sqrt{2}}(|+2\rangle - |-2\rangle) \end{aligned} \quad (1)$$

Finally, the $\pm 45^\circ$ angle “antidiagonal” and “diagonal” linear polarizations are hereafter denoted with the kets $|A\rangle = (|H\rangle + |V\rangle)/\sqrt{2}$ and $|D\rangle = (|H\rangle - |V\rangle)/\sqrt{2}$, and the corresponding OAM states are defined analogously:

$$\begin{aligned} |a\rangle &= \frac{1}{\sqrt{2}}(|h\rangle + |v\rangle) = \frac{e^{-i\pi/4}}{\sqrt{2}}(|+2\rangle + i|-2\rangle), \\ |d\rangle &= \frac{1}{\sqrt{2}}(|h\rangle - |v\rangle) = \frac{e^{i\pi/4}}{\sqrt{2}}(|+2\rangle - i|-2\rangle). \end{aligned} \quad (2)$$

Since we deal with a four-dimensional Hilbert space, the complete characterization of a ququart state is achieved by defining and measuring five mutually unbiased bases with four states each [45,46]. Indeed a density matrix of a d -dimensional quantum system, with d expressed as a prime power, can be completely reconstructed from the measurements with respect to $d + 1$ mutually unbiased bases [47]. The 20 states composing the five mutually unbiased bases, denoted as I, II, III, IV, and V, are reported in Table I both in the ququart logic basis as well as in the OAM-polarization nomenclature. Let us stress that while bases I, II, and III correspond to the measurement of $\sigma_z \otimes \tilde{\sigma}_z$, $\sigma_x \otimes \tilde{\sigma}_x$, and $\sigma_y \otimes \tilde{\sigma}_y$ on the two-qubit systems (where the tilde denotes the Pauli operator for OAM states), the bases IV and V refer to entangled states between polarization and OAM.

III. QUQUART MANIPULATION VIA q PLATE

The main feature of the q plate is its capability of coupling the spinorial (polarization) and orbital contributions of the angular momentum of photons. A q plate (QP) is a birefringent slab having a suitably patterned transverse optical axis, with

a topological singularity at its center [43]. The “charge” of this singularity is given by an integer or half-integer number q , which is determined by the (fixed) pattern of the optical axis. The birefringent retardation δ_{QP} must instead be uniform across the device. For $\delta_{QP} = \pi$, a QP modifies the OAM state m of a light beam crossing it, imposing a variation $\Delta m = \pm 2q$ whose sign depends on the input polarization (positive for left-circular and negative for right-circular). On the polarization degree of freedom, the q plate acts as a half-wave plate. In the present work, we use QPs with charge $q = 1$ and retardation $\delta = \pi$. Hence, an input TEM₀₀ mode (having $m = 0$) is converted into a beam with $m = \pm 2$:

$$\begin{aligned} |L\rangle_\pi |0\rangle_o &\xrightarrow{QP} |R\rangle_\pi |+2\rangle_{o_2}, \\ |R\rangle_\pi |0\rangle_o &\xrightarrow{QP} |L\rangle_\pi |-2\rangle_{o_2}, \end{aligned} \quad (3)$$

where L and R denote the left and right circular polarization states, respectively. It has been experimentally demonstrated that any coherent superposition of the two input states given in Eq. (3) is preserved by the QP transformation, leading to the equivalent superposition of the corresponding output states [44]. Hence, the QP can be easily employed to generate single-particle entanglement of π and OAM degrees of freedom, a property that can be exploited to generate ququart states in the entangled mutually unbiased bases IV and V. Such a property, experimentally verified in [44], can be synthetically expressed as follows:

$$\begin{Bmatrix} |H\rangle_\pi |0\rangle_o \\ |V\rangle_\pi |0\rangle_o \end{Bmatrix} \xleftrightarrow{QP} \frac{1}{\sqrt{2}}(|L\rangle_\pi |-2\rangle_{o_2} \pm |R\rangle_\pi |+2\rangle_{o_2}). \quad (4)$$

This is an entangled state between two qubits encoded in different degrees of freedom belonging to the mutually unbiased basis IV for ququart states. Thus, the ability of the q plate to *entangle-disentangle* the OAM-polarization degrees of freedom is exploited for the preparation as well as for the measurement of the ququart states. For the preparation and analysis stages, let us refer to Fig. 1.

A. Preparation stage

The states belonging to bases I, II, and III are generated through the transferrer $\pi \rightarrow o_2$, which achieves the transformation $|\varphi\rangle_\pi |0\rangle_o \rightarrow |H\rangle_\pi |\varphi\rangle_{o_2}$, where $|0\rangle_o$ denotes the zero-OAM state. This transferrer, presented in [44,48], is based on two wave plates, a q plate and a polarizing beam splitter, thus allowing the coherent transfer of the information initially encoded in the polarization to the OAM degree of freedom. After the transferrer $\pi \rightarrow o_2$ it is possible to encode new information in the polarization by adopting two wave plates. The preparation stage for states belonging to bases IV and V is based on two wave plates and a q plate, which allow transformations analogous to the one in Eq. (4) to be achieved, depending on the polarization state initially encoded through the wave plates. The half-wave plate δ (shown in Fig. 1) can be inserted depending on the specific state to be prepared. In Table I, the rotations of the wave plates in the preparation stage to be applied for the generation of all the ququart states are reported. We note that by this method we can generate all ququarts belonging to the five unbiased bases, but not an arbitrary ququart. The latter could be obtained

TABLE I. Mutually unbiased bases for ququart states expressed in the logic ququart basis $|1\rangle, |2\rangle, |3\rangle, |4\rangle$ and in terms of polarization and orbital angular momentum. On the right-hand side of the table are reported the different settings of the wave plates (see Fig. 1) for the experimental preparation and analysis of the ququart states through the q -plate device. These settings correspond to the optical axis angle with respect to the horizontal laboratory axis, assuming that the input photon state is $|H\rangle_\pi |0\rangle_o$. In the last column on the right are reported the overall experimental fidelities including both the preparation and the measurement stages. The uncertainties have been evaluated according to the Poissonian statistics of the photon counting.

Theory			Experimental implementation through the q -plate device										
Ququart states			Preparation				Analysis						F_{expt}
Ququart logic bases	OAM- π		α	β	γ	δ	ϵ	φ	λ	τ	χ	μ	
I	$ 1\rangle$	$ H, +2\rangle$	-45	0	0	0	0	0	-45	+45	0	0	$(99.9 \pm 0.4)\%$
	$ 2\rangle$	$ H, -2\rangle$	+45	0	0	0	0	0	-45	+45	0	+45	$(94.6 \pm 0.4)\%$
	$ 3\rangle$	$ V, +2\rangle$	-45	0	0	+45	0	+45	-45	+45	0	0	$(99.9 \pm 0.4)\%$
	$ 4\rangle$	$ V, -2\rangle$	+45	0	0	+45	0	+45	-45	+45	0	+45	$(95.8 \pm 0.4)\%$
II	$\frac{1}{2}(1\rangle + 2\rangle + 3\rangle + 4\rangle)$	$ A, h\rangle$	0	0	0	+22.5	+45	+22.5	-45	+45	+45	+22.5	$(95.0 \pm 0.4)\%$
	$\frac{1}{2}(1\rangle - 2\rangle + 3\rangle - 4\rangle)$	$ A, v\rangle$	0	+45	0	+22.5	+45	+22.5	-45	+45	+45	+22.5	$(89.2 \pm 0.4)\%$
	$\frac{1}{2}(1\rangle + 2\rangle - 3\rangle - 4\rangle)$	$ D, h\rangle$	0	0	0	-22.5	+45	-22.5	-45	+45	+45	-22.5	$(97.7 \pm 0.4)\%$
	$\frac{1}{2}(1\rangle - 2\rangle - 3\rangle + 4\rangle)$	$ D, v\rangle$	+45	0	0	-22.5	+45	-22.5	-45	+45	+45	-22.5	$(95.0 \pm 0.4)\%$
III	$\frac{1}{2}(1\rangle + i 2\rangle + i 3\rangle - 4\rangle)$	$ R, a\rangle$	0	-22.5	+45	0	+45	0	-45	+45	+45	0	$(96.3 \pm 0.4)\%$
	$\frac{1}{2}(1\rangle - i 2\rangle + i 3\rangle + 4\rangle)$	$ R, d\rangle$	0	+22.5	+45	0	+45	0	-45	+45	+45	0	$(95.7 \pm 0.4)\%$
	$\frac{1}{2}(1\rangle + i 2\rangle - i 3\rangle + 4\rangle)$	$ L, a\rangle$	0	-22.5	-45	+45	-45	0	-45	+45	-45	0	$(94.1 \pm 0.4)\%$
	$\frac{1}{2}(1\rangle - i 2\rangle - i 3\rangle - 4\rangle)$	$ L, d\rangle$	0	+22.5	-45	+45	-45	0	-45	+45	-45	0	$(94.5 \pm 0.4)\%$
IV	$\frac{1}{2}(1\rangle + 2\rangle + i 3\rangle - i 4\rangle)$	$\frac{1}{\sqrt{2}}(R, +2\rangle + L, -2\rangle)$	0	0						0	0	0	$(84.8 \pm 0.4)\%$
	$\frac{1}{2}(1\rangle - 2\rangle + i 3\rangle + i 4\rangle)$	$\frac{1}{\sqrt{2}}(R, +2\rangle - L, -2\rangle)$	0	+45						0	0	+45	$(91.4 \pm 0.4)\%$
	$\frac{1}{2}(1\rangle + 2\rangle - i 3\rangle + i 4\rangle)$	$\frac{1}{\sqrt{2}}(L, +2\rangle + R, -2\rangle)$	0	0		+45		0		0	0	0	$(89.4 \pm 0.4)\%$
	$\frac{1}{2}(1\rangle - 2\rangle - i 3\rangle - i 4\rangle)$	$\frac{1}{\sqrt{2}}(L, +2\rangle - R, -2\rangle)$	0	+45		+45		0		0	0	+45	$(88.4 \pm 0.4)\%$
V	$\frac{1}{2}(1\rangle + i 2\rangle + 3\rangle - i 4\rangle)$	$\frac{1}{\sqrt{2}}(H, a\rangle + V, d\rangle)$	0	+22.5			+45		-45	+45	+45	+22.5	$(89.7 \pm 0.4)\%$
	$\frac{1}{2}(1\rangle + i 2\rangle - 3\rangle + i 4\rangle)$	$\frac{1}{\sqrt{2}}(H, a\rangle - V, d\rangle)$	0	-22.5			+45		-45	+45	+45	-22.5	$(86.1 \pm 0.4)\%$
	$\frac{1}{2}(1\rangle - i 2\rangle + 3\rangle + i 4\rangle)$	$\frac{1}{\sqrt{2}}(H, d\rangle + V, a\rangle)$	0	+22.5		+45	+45	0	-45	+45	+45	+22.5	$(88.4 \pm 0.4)\%$
	$\frac{1}{2}(1\rangle - i 2\rangle - 3\rangle - i 4\rangle)$	$\frac{1}{\sqrt{2}}(H, d\rangle - V, a\rangle)$	0	-22.5		+45	+45	0	-45	+45	+45	-22.5	$(92.0 \pm 0.4)\%$

by implementing the more complex universal unitary gate proposed in [49]. However, to demonstrate the generality of any quantum protocol, it is enough to test it on all states belonging to a complete set of unbiased bases, such as those generated in the present work.

B. Analysis stage

The measurement procedure of the ququart states depends on the bases to be analysed. The schemes are reported in Fig. 1 (right-hand side). The states belonging to bases I, II, and III have been measured first in the polarization contribution of the wave function through a standard polarization analysis set composed of two wave plates and a polarizing beam splitter (PBS). Then the orbital contribution has been analyzed, adopting the quantum transferrer $o_2 \rightarrow \pi$, which achieves the transformation $|H\rangle_\pi |\varphi\rangle_{o_2} \Rightarrow |\varphi\rangle_\pi |0\rangle_o$ [44,48]. Such a transferrer is based on a q plate, two wave plates, and a single-mode fiber which selects only the orbital contributions with $m = 0$. Hence, this analysis stage is a probabilistic one, with $p = 0.5$. After the transferrer, the state $|\varphi\rangle_\pi |0\rangle_o$ has

been measured through a standard polarization analysis set. Two multimode fibers collect the output signals of the PBS and then send them to the detectors, as described in detail in the experimental section. States belonging to bases IV and V have been measured, exploiting the q -plate capability of disentangling the polarization from the OAM degree of freedom. Thus, depending on the state to be analyzed, two wave plates have been inserted in order to manipulate the polarization component of the wave function, and then the state has been sent through the $o_2 \rightarrow \pi$ transferrer. Finally, the output state from the single-mode fiber has been measured through a standard polarization analysis set, as for states belonging to bases I, II, and III. Let us stress that this detection stage is also a probabilistic one, with $p = 0.5$.

Nevertheless, it is possible to realize two fully *deterministic* transferrers $\pi \rightarrow o_2$ and $o_2 \rightarrow \pi$ at the price of a more complex optical layout, based on a q plate and a Sagnac interferometer, as shown in [48]. This result can be applied in order to achieve a deterministic preparation stage for all the bases (I, II, III, IV, and V) and a deterministic measurement stage for bases I, II, and III.

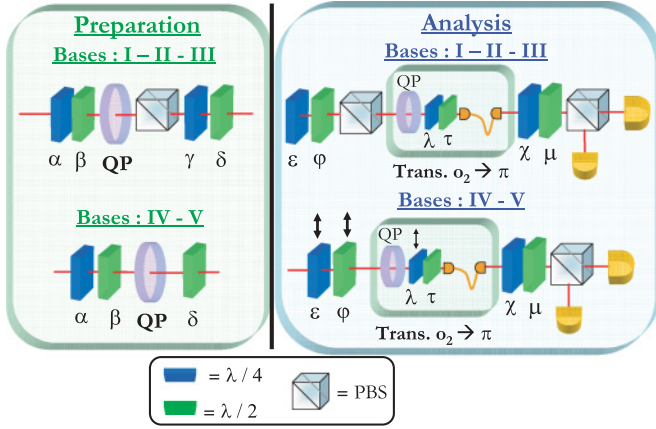


FIG. 1. (Color online) Schematic representation of the preparation and analysis setting stages of the ququart states adopted in our experiment. The preparation stages of the bases I, II, and III works with probability equal to 50%; however, a deterministic implementation can be achieved by adopting the scheme proposed in [48]. The preparation stages for states IV and V are deterministic. All the analysis schemes are probabilistic with $p = 50\%$, but the setup for states I, II, and III can again be made deterministic by exploiting the $o_2 \rightarrow \pi$ transferrer proposed in [44,48].

In Fig. 2 we propose two schemes in order to analyze deterministically all the ququart states belonging to the five mutually unbiased bases. In particular, states of bases IV and V can be measured with $p = 1$ by inserting a controlled-NOT scheme where the polarization controls the OAM degree of freedom. Depending on the π contribution of the wave function, in the Sagnac interferometer a σ_z operator, implemented through a Dove prism (DP) properly rotated, acts on the orbital degree of freedom. Hence, the state is analyzed in polarization and then in OAM by the deterministic $o_2 \rightarrow \pi$ transferrer. It is worth noting that the schemes proposed here can be adopted in order to carry out a quantum Bell state measurement of a hybrid ququart state encoded in polarization and OAM.

IV. EXPERIMENTAL CHARACTERIZATION

The experimental layout is shown in Fig. 3. A β -barium borate (BBO) crystal cut for type II phase matching, pumped by the second harmonic of a Ti:sapphire mode-locked laser beam, generates photon pairs via spontaneous parametric fluorescence on modes k_A and k_B with linear polarization, wavelength $\lambda = 795$ nm, and pulse bandwidth $\Delta\lambda = 4.5$ nm, as determined by two interference filters (IFs). The coincidence rate of the source is equal to 8 kHz. The photon generated on mode k_A is detected at D_T , thus acting as a trigger on the single-photon generation. The photon generated on mode k_B is delivered to the setup via a single-mode fiber, thus defining its transverse spatial mode to a pure TEM_{00} , corresponding to OAM $m = 0$. After the fiber output, two wave plates compensate (C) the polarization rotation introduced by the fiber. Then the ququart is encoded in the single-photon polarization and OAM through the ququart preparation stage, whose structure depends on the state to be generated, as described in the previous section. After the ququart analysis stage, the output photons have been

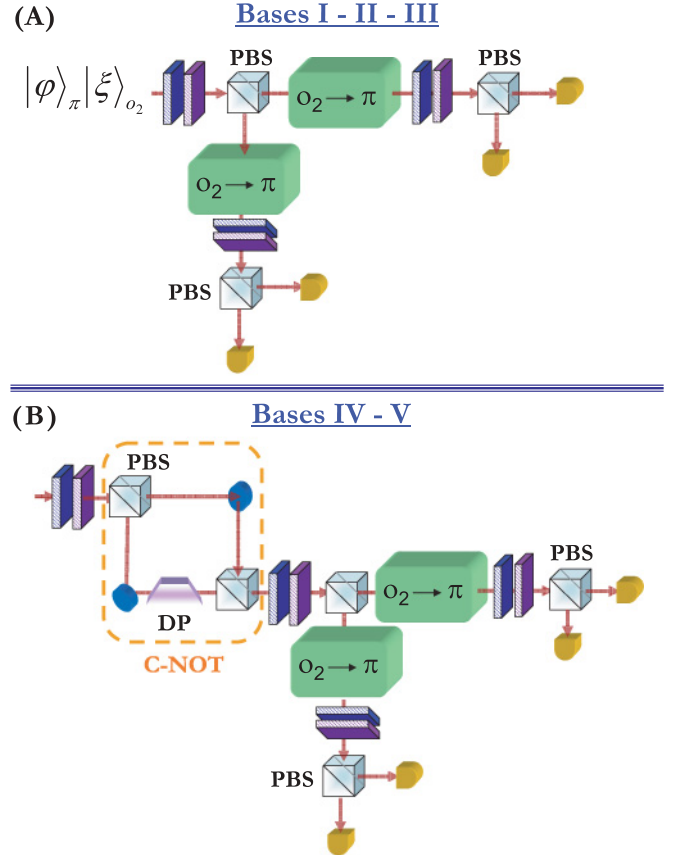


FIG. 2. (Color online) Schematic representation of the deterministic analysis setting stages of the ququart states belonging to (a) bases I, II, and III and (b) bases IV and V. The $o_2 \rightarrow \pi$ transferrer in both schemes works deterministically, as proposed in [48].

coupled to single-mode fibers and then detected by two single-photon counter modules connected to the coincidence box, which records the coincidence counts between $[D_1, D_T]$ and $[D_2, D_T]$. For the detailed representation of the preparation and analysis ququart stages, let us refer to Fig. 1.

As first step, we have estimated the fidelities for all quantum states of the five mutually unbiased bases. The experimental fidelities F_{expt} are reported in Table I. For every input state $|\varphi\rangle$, F_{expt} has been estimated as $F_{\text{expt}} = \frac{p(|\varphi\rangle)}{\sum_i p(|\psi_i\rangle)}$, where $p(|\psi_i\rangle)$ is the probability to detect $|\psi_i\rangle$. The average value \bar{F} for each basis reads as follows:

Basis	$\bar{F}(\%)$
I	97.6 ± 0.4
II	94.2 ± 0.4
III	95.2 ± 0.4
IV	88.5 ± 0.4
V	89.1 ± 0.4

These values take into account the fidelity of both preparation and measurement steps. Since these two processes are fairly symmetrical, the fidelities associated with the single preparation or measurement stage can be estimated as the square root of the previous values.

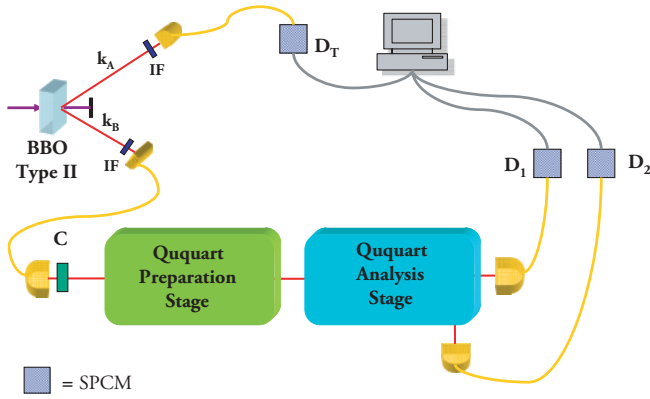


FIG. 3. (Color online) Experimental setup adopted for the generation and characterization of ququart states encoded in the polarization and orbital angular momentum of a single photon.

As can be observed from the preceding table, there is a slight difference ($\sim 6\%$) between the mean fidelity value of states belonging to the first three bases and the one related to states of bases IV and V. Indeed a discrepancy of around 3% is shown for the present limitation of the efficiency, which implies small random contributions to the polarization after the generation

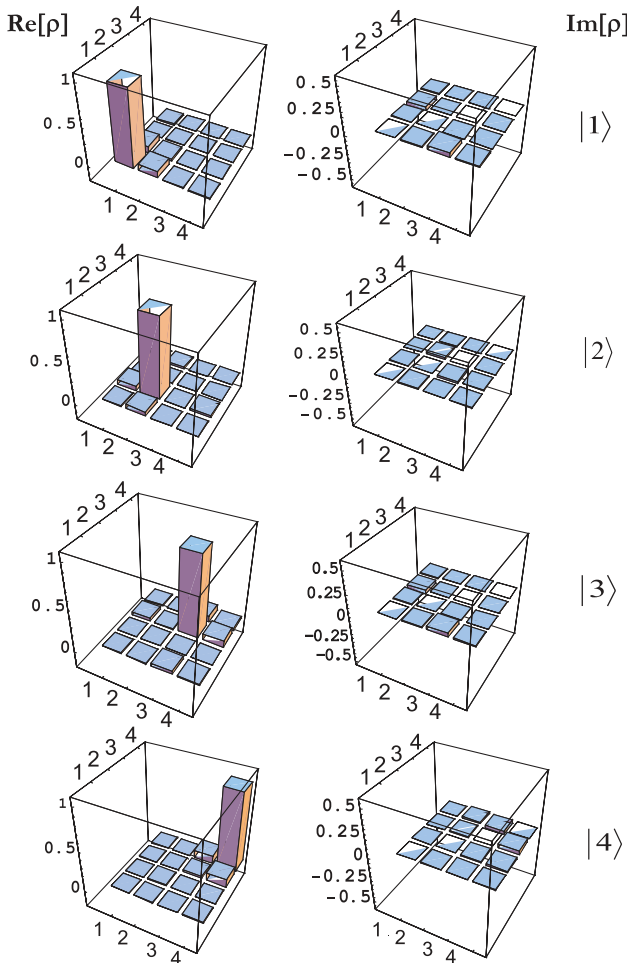


FIG. 4. (Color online) Experimental density matrices of ququart states belonging to the first mutually unbiased basis. The states $|1\rangle, |2\rangle, |3\rangle, |4\rangle$ are reported on axis, schematically written as 1,2,3,4. The elements of the density matrix are reported on the ordinate.

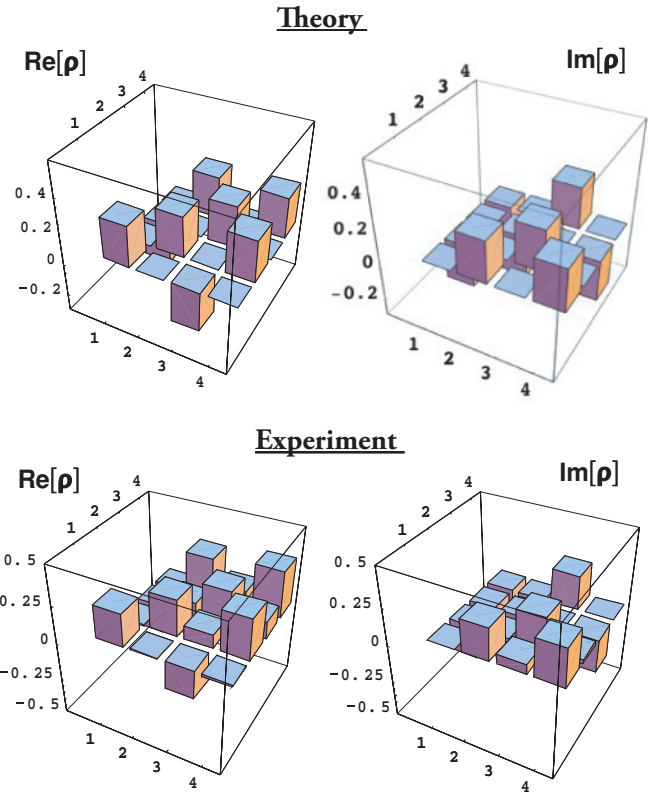


FIG. 5. (Color online) Theoretical and experimental density matrix of a ququart state belonging to the fifth mutually unbiased basis. The state reported is $(2^{1/2})(|H,d\rangle - |V,a\rangle)$. The states $|1\rangle, |2\rangle, |3\rangle, |4\rangle$ are reported on axis, schematically written as 1,2,3,4. The elements of the density matrix are reported on the coordinate.

of the ququart states. Since for the analysis of entangled states between π and OAM the polarizing beam splitter was removed, such unconverted contributions are not filtered and thus affect the final fidelity. The remaining 3% is due to phase effects between different contributions in the entangled π -OAM wave function, as well as a slight misalignment with respect to the separable states experimental setup.

V. QUANTUM-STATE TOMOGRAPHY OF QUQUART

The ability to prepare the ququart codified in the OAM-polarization space in all the mutually unbiased bases has been experimentally verified by reconstructing their density matrices through quantum-state tomography. The experimental density matrix associated with a ququart can be expressed as

$$\hat{\rho} = \frac{1}{4} \sum_{j=1}^{d^2=16} r_j \hat{\lambda}_j, \quad (5)$$

where $\{\hat{\lambda}_j\}$ is a complete operatorial set of Hermitian generators and $r_j = \langle \hat{\lambda}_j \rangle = \text{Tr}[\hat{\rho} \hat{\lambda}_j]$.

The set of operators $\{\hat{\lambda}_j\}$ for the ququart considered here can be obtained by starting from the generators of $\text{SU}(2)$ as $\text{SU}(2) \otimes \text{SU}(2)$: $\hat{\sigma}_i^\pi \otimes \hat{\sigma}_j^{\text{OAM}}$. The tomography reconstruction obtained in the following way requires the estimation of

TABLE II. Fidelity and linear entropy of experimental ququart states belonging to all five mutually unbiased bases.

Input states	$F(\%)$	S_L
$ H, -2\rangle$	98.5 ± 0.3	0.058 ± 0.002
$ A, v\rangle$	90.5 ± 0.3	0.046 ± 0.002
$ L, a\rangle$	95.4 ± 0.3	0.097 ± 0.002
$\frac{1}{\sqrt{2}}(R, +2\rangle - L, -2\rangle)$	93.0 ± 0.3	0.092 ± 0.002
$\frac{1}{\sqrt{2}}(H, a\rangle - V, d\rangle)$	92.0 ± 0.3	0.094 ± 0.002

16 operators [50] through 36 separable measurements on the polarization-OAM subspaces:

$$\begin{aligned}
\hat{\lambda}_1 &= \hat{\sigma}_X \otimes \hat{I}, & \hat{\lambda}_9 &= \hat{\sigma}_X \otimes \hat{\sigma}_Y \\
\hat{\lambda}_2 &= \hat{\sigma}_Y \otimes \hat{I}, & \hat{\lambda}_{10} &= \hat{\sigma}_Y \otimes \hat{\sigma}_Y \\
\hat{\lambda}_3 &= \hat{\sigma}_Z \otimes \hat{I}, & \hat{\lambda}_{11} &= \hat{\sigma}_Z \otimes \hat{\sigma}_Y \\
\hat{\lambda}_4 &= \hat{I} \otimes \hat{\sigma}_X, & \hat{\lambda}_{12} &= \hat{I} \otimes \hat{\sigma}_Z \\
\hat{\lambda}_5 &= \hat{\sigma}_X \otimes \hat{\sigma}_X, & \hat{\lambda}_{13} &= \hat{\sigma}_X \otimes \hat{\sigma}_Z \\
\hat{\lambda}_6 &= \hat{\sigma}_Y \otimes \hat{\sigma}_X, & \hat{\lambda}_{14} &= \hat{\sigma}_Y \otimes \hat{\sigma}_Z \\
\hat{\lambda}_7 &= \hat{\sigma}_Z \otimes \hat{\sigma}_X, & \hat{\lambda}_{15} &= \hat{\sigma}_Z \otimes \hat{\sigma}_Z \\
\hat{\lambda}_8 &= \hat{I} \otimes \hat{\sigma}_Y, & \hat{\lambda}_{16} &= \hat{I} \otimes \hat{I}.
\end{aligned}$$

We carried out the reconstruction of ρ for different states belonging to all the bases previously introduced. Examples of the experimental results are reported in Figs. 4 and 5. The accordance between theory and experiment can be appreciated by looking at the tomographies as well as through the fidelity $F = \langle \phi | \rho | \phi \rangle$ and the linear entropy (S_L) values, theoretically equal to zero, with the ideal states evaluated for some states belonging to the five mutually unbiased basis (see Table II):

Let us stress that the adoption of the q plate has also allowed the reconstruction of the density matrix for the states belonging to the fourth and fifth basis, related to entangled states between orbital angular momentum and polarization of a single photon.

The previous approach requires the measurements of 16 operators and the corresponding 64 eigenstates. A more

efficient quantum-state reconstruction could be achieved by adopting all the mutually unbiased bases as just proposed and demonstrated with a two-photon system in [51]. The reduced number of bases in a mutually unbiased basis tomography allows the number of measurements to achieve the same reconstruction accuracy to be reduced by a factor of 5/9. Moreover, this technique turned out to be even more efficient for entangled states since it directly estimates the strength of correlations in entangled bases (IV and V) [51].

VI. CONCLUSION

In this paper we have experimentally carried out the encoding of a ququart state in the polarization and orbital angular momentum of a single photon. The states generated have been fully characterized through quantum-state tomography by measuring all five mutually unbiased bases expected in a four-dimensional Hilbert space. The capacity to manipulate with high reliability all ququart states encoded in a single photon enforce the achievement of the quantum-state engineering of ququart to be directed toward the implementation of new quantum information protocols and more robust communication procedures. In particular, single-photon encoded ququart states could be adopted for the implementation of a quantum key distribution protocol without a reference frame, which was recently proposed [21,22], as well as for the implementation of a universal unitary gate [49]. Finally, the advantage of encoding a ququart state in a single photon could be exploited for quantum information protocols like the optimal quantum cloning of quantum states with dimension $d > 2$ [37].

ACKNOWLEDGMENTS

E.N. and F.S. acknowledge support by the FARI project and Finanziamento Ateneo 2009 of Sapienza Università di Roma.

-
- [1] N. J. Cerf, M. Bourennane, A. Karlsson, and N. Gisin, *Phys. Rev. Lett.* **88**, 127902 (2002).
- [2] B. P. Lanyon, M. Barbieri, M. P. Almeida, T. Jennewein, T. C. Ralph, K. J. Resch, G. J. Pryde, J. L. O'Brien, A. Gilchrist, and A. G. White, *Nature Phys.* **5**, 134 (2009).
- [3] D. Collins, N. Gisin, N. Linden, S. Massar, and S. Popescu, *Phys. Rev. Lett.* **88**, 040404 (2002).
- [4] D. Kaszlikowski, P. Gnacinski, M. Zukowski, W. Miklaszewski, and A. Zeilinger, *Phys. Rev. Lett.* **85**, 4418 (2000).
- [5] D. Kaszlikowski, L. C. Kwek, J. L. Chen, M. Zukowski, and C. H. Oh, *Phys. Rev. A* **65**, 032118 (2002).
- [6] M. Genovese, *Phys. Rep.* **413**, 319 (2005).
- [7] T. Vertesi, S. Pironio, and N. Brunner, e-print arXiv:0909.3171v1.
- [8] X. Wang, B. C. Sanders, and D. W. Berry, *Phys. Rev. A* **67**, 042323 (2003).
- [9] R. Jozsa and J. Schlienz, *Phys. Rev. A* **62**, 012301 (2000).
- [10] D. P. DiVincenzo, T. Mor, P. W. Shor, J. A. Smolin, and B. M. Terhal, *Commun. Math. Phys.* **238**, 379 (2003).
- [11] J. Joo, P. L. Knight, J. L. O'Brien, and T. Rudolph, *Phys. Rev. A* **76**, 052326 (2007).
- [12] M. Fujiwara, M. Takeoka, J. Mizuno, and M. Sasaki, *Phys. Rev. Lett.* **90**, 167906 (2003).
- [13] C. Allen Bishop and M. S. Byrd, *J. Phys. A* **42**, 055301 (2009).
- [14] H. Bechmann-Pasquinucci and A. Peres, *Phys. Rev. Lett.* **85**, 3313 (2000).
- [15] M. Bourennane, A. Karlsson, and G. Bjork, *Phys. Rev. A* **64**, 012306 (2001).
- [16] N. Gisin, G. Ribordy, W. Tittel, and H. Zbinden, *Rev. Mod. Phys.* **74**, 145 (2002).
- [17] D. Bruss and C. Macchiavello, *Phys. Rev. Lett.* **88**, 127901 (2002).
- [18] S. P. Walborn, D. S. Lemelle, M. P. Almeida, and P. H. Souto Ribeiro, *Phys. Rev. Lett.* **96**, 090501 (2006).
- [19] S. P. Kulik and A. P. Shurupov, *J. Exp. Theor. Phys.* **104**, 736 (2006).
- [20] S. P. Kulik, G. A. Maslennikov, and E. V. Moreva, *J. Exp. Theor. Phys.* **102**, 712 (2006).

- [21] C. E. R. Souza, C. V. S. Borges, A. Z. Khoury, J. A. O. Huguenin, L. Aolita, and S. P. Walborn, *Phys. Rev. A* **77**, 032345 (2008).
- [22] A. P. Shurupov, S. S. Straupe, S. P. Kulik, M. Gharib, and M. R. B. Wahiddin, *Europhys. Lett.* **87**, 10008 (2009).
- [23] T. C. Ralph, K. J. Resch, and A. Gilchrist, *Phys. Rev. A* **75**, 022313 (2007).
- [24] K. S. Ranade, *Phys. Rev. A* **80**, 022301 (2009).
- [25] G. Benenti and G. Strini, *Phys. Rev. A* **79**, 052301 (2009).
- [26] Yongmin Li, Kuanshou Zhang, and Kunchi Peng, *Phys. Rev. A* **77**, 015802 (2008).
- [27] M. Neeley, M. Ansmann, R. C. Bialczak, M. Hofheinz, E. Lucero, A. D. O'Connell, D. Sank, H. Wang, J. Wenner, A. N. Cleland, M. R. Geller, and J. M. Martinis, *Science* **325**, 722 (2009).
- [28] B. P. Lanyon, T. J. Weinhold, N. K. Langford, J. L. O'Brien, K. J. Resch, A. Gilchrist, and A. G. White, *Phys. Rev. Lett.* **100**, 060504 (2008).
- [29] S. Y. Baek, S. S. Straupe, A. P. Shurupov, S. P. Kulik, and Y. H. Kim, *Phys. Rev. A* **78**, 042321 (2008).
- [30] G. M. D'Ariano, P. Mataloni, and M. F. Sacchi, *Phys. Rev. A* **71**, 062337 (2005).
- [31] E. V. Moreva, G. A. Maslennikov, S. S. Straupe, and S. P. Kulik, *Phys. Rev. Lett.* **97**, 023602 (2006).
- [32] Y. I. Bogdanov, E. V. Moreva, G. A. Maslennikov, R. F. Galeev, S. S. Straupe, and S. P. Kulik, *Phys. Rev. A* **73**, 063810 (2006).
- [33] G. Vallone, E. Pomarico, F. De Martini, P. Mataloni, and M. Barbieri, *Phys. Rev. A* **76**, 012319 (2007).
- [34] S. Y. Baek and Y. H. Kim, *Phys. Rev. A* **75**, 034309 (2007).
- [35] S. Franke-Arnold, L. Allen, and M. Padgett, *Laser Photon. Rev.* **2**, 299 (2008).
- [36] G. Molina-Terriza, J. P. Torres, and L. Torner, *Nature Phys.* **3**, 305 (2007).
- [37] E. Nagali, L. S. Sciarrino, F. De Martini, L. Marrucci, B. Piccirillo, E. Karimi, and E. Santamato, *Nature Photonics* **3**, 720 (2009).
- [38] J. P. Torres, Y. Deyanova, L. Torner, and G. Molina-Terriza, *Phys. Rev. A* **67**, 052313 (2003).
- [39] A. Vaziri, J. W. Pan, T. Jennewein, G. Weihs, and A. Zeilinger, *Phys. Rev. Lett.* **91**, 227902 (2003).
- [40] G. Molina-Terriza, A. Vaziri, J. Reháček, Z. Hradil, and A. Zeilinger, *Phys. Rev. Lett.* **92**, 167903 (2004).
- [41] G. Molina-Terriza, A. Vaziri, R. Ursin, and A. Zeilinger, *Phys. Rev. Lett.* **94**, 040501 (2005).
- [42] N. K. Langford, R. B. Dalton, M. D. Harvey, J. L. O'Brien, G. J. Pryde, A. Gilchrist, S. D. Bartlett, and A. G. White, *Phys. Rev. Lett.* **93**, 053601 (2004).
- [43] L. Marrucci, C. Manzo, and D. Paparo, *Phys. Rev. Lett.* **96**, 163905 (2006).
- [44] E. Nagali, F. Sciarrino, F. De Martini, L. Marrucci, B. Piccirillo, E. Karimi, and E. Santamato, *Phys. Rev. Lett.* **103**, 013601 (2009).
- [45] A. Klappenecker and M. Rotteler, *Lect. Notes Comput. Sci.* **2984**, 137 (2004).
- [46] M. Planat and A. C. Baboin, *J. Phys. A* **40** F1005 (2007).
- [47] I. D. Ivanovic, *J. Phys. A* **14**, 3241 (1981).
- [48] E. Nagali, F. Sciarrino, F. De Martini, L. Marrucci, B. Piccirillo, E. Karimi, and E. Santamato, *Opt. Express* **17**, 18745 (2009).
- [49] S. Slussarenko, E. Karimi, B. Piccirillo, L. Marrucci, and E. Santamato, *Phys. Rev. A* **80**, 022326 (2009).
- [50] D. F. V. James, P. G. Kwiat, W. J. Munro, and A. G. White, *Phys. Rev. A* **64**, 052312 (2001).
- [51] R. B. A. Adamson and A. M. Steinberg, e-print [arXiv:0808.0944](https://arxiv.org/abs/0808.0944) [quant-ph].